B.I. LEV, V.B. TYMCHYSHYN, A.G. ZAGORODNY

Bogolyubov Institute for Theoretical Physics, Nat. Acad. of Sci. of Ukraine
(14b, Metrolohichna Str., Kyiv 03680, Ukraine; e-mail: blev@bitp.kiev.ua, yu.binkukoku@gmail.com, azagorodny@bitp.kiev.ua)

POTENTIAL ENERGY ANALYSIS FOR A SYSTEM OF INTERACTING PARTICLES ARRANGED IN A BRAVAIS LATTICE

PACS 52.27.Lw, 02.30.Mv

We propose a method to calculate the type of a lattice formed by grains in dusty plasma and estimate its potential energy. Basically, this task is complicated by the interparticle potential that appertains to "catastrophic potentials". This kind of potentials needs special approaches to avoid divergences during potential energy calculations. In the current contribution, we will develop all the necessary modifications to appropriate methods. It will be shown that the obtained potential energy expression can be used to determine lattice parameters and these parameters comply to known experimental data.

K e y w o r d s: Coulomb potential, dusty plasma, potential energy, Bravais lattice.

1. Introduction

There are many soft-matter systems such as grains in a dusty plasma, colloids in various solvents, surfactant solutions, *etc.*, that exhibit the self-organization and rearrangement in crystalline structures under certain conditions. They are often described with a Coulomb-like long-range potential. Thus, on one hand, we have very interesting physical systems with applications to the studies of a variety of peculiar phenomena in different fields of science [1–3]. On the other hand, we have interaction that leads to a divergence during potential energy calculations (that is why they are often called "catastrophic potentials") and highly complicates the consideration. This induced a variety of successful approaches to treat divergences [4–10].

If we overcome the infinite energy problem somehow, then the partition function will be exactly evaluated only for few model systems of interacting particles in the thermodynamical limit [9, 11–15]. But that is the case where one can observe crystallization-like phenomena and transitions between different lattice symmetries [16–20], which is the case of study.

This work is based on Ewald's sum modification. In particular, instead of describing particle's position with the delta-function, a certain distribution function will be used. This approach is known, because it

allows one to consider the boundary effects for finite particles' clusters [4,9] and to obtain some progress in potential energy calculations for two-dimensional systems [11]. Namely, we will expand and significantly supplement results obtained for two dimensions in [11], by making them applicable to three-dimensional systems. It will be shown that the three-dimensional case is more complicated, but, instead, we can perform the significant convergence improvement for series representing the potential energy of a Coulomb-like system.

In Section 4, we will consider grains in dusty plasma and apply the developed methods to find the expected lattice and compare it to known experimental data. It was chosen as the one manifesting a lot of interesting effects. For example, dusty plasma may serve as a perfect medium for the experimental exploration of classical fluids and solids along with colloids [20, 22–30].

Along this article, one will meet *examples* after each block of calculations in Section 2. They serve two purposes. First of all, they show how to use the introduced equations in some practical case. The second purpose is reuse of results obtained in *examples*, when treating dusty plasma in Section 4. Depending on personal preferences, one may read them in the given order, as well as skip and then return, when they are referenced in Section 4.

For the current article not to be overloaded with lots and lots of complicated mathematical compu-
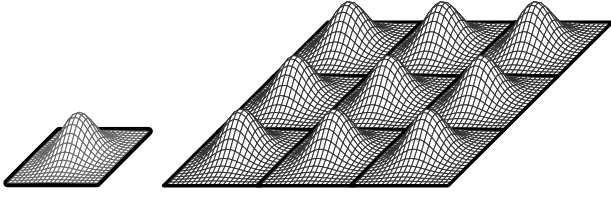
Fig. 1. Two-dimensional analogy of the transition from a single-particle probability distribution function $\rho_{\mathrm{sp}}(\mathbf{r})$ (on the left) to the many-particle one $\rho(\mathbf{r})$ (on the right). Function $\rho(\mathbf{r})$ is defined for all $\mathbb{R}^2$ with two-dimensional analogy of (1)

tations, we moved them to *appendices* 5. Thus, it mostly contains some physical explanations and results. But using references to *appendices*, one may find here the detailed rigorous exposition of the presented ideas as well.

The rest of the article is organized as follows. It can be contingently divided into two parts: development of a technique and its application. Section 2 focuses on a general expression for the potential energy for any Bravais lattice and any potential. In addition, the most interesting case of Coulomb potential is considered to show how to use the developed technique.

In Section 3, we will analyze possible uncertainties in the choice of lattice parameters and eliminate them. This is very important, because the minimization algorithm starts often with very large parameters, when the lattice can be described with much smaller numbers. In this case, the calculation errors emerge and computer starts getting wrong results for the potential energy, which makes this calculation unstable and incorrect. Thus, in Section 3, we provide a method to avoid the mentioned problem during the minimization process.

In the last section 4, a crystal of dust particles is considered. It is shown that the hexagonal close packing seems to be the lattice we expect to be seen in experiment. This is in agreement with experiments [16] and computer simulations [17]. One more interesting conclusion we get is that the lattice type is independent of the grain charge.

2. Particles Arranged in a Lattice

In this section, we aim to find a method of potential energy calculation for a system of identical (from potential's point of view) particles arranged in a Bravais lattice.

As a result, we will get an expression for the potential energy in the form of series (6). If the potential

approaches the "catastrophic" one, the mentioned series may contain at most one diverging term. This term does not depend on any lattice parameter but the mean particle number density only. Thus, there are plenty of problems, where we can use this term as energy's "ground-level" (similar to the renormalization approach in QFT).

2.1. Particle's spatial distribution function

Suppose we have an equilibrium static multiparticle system in the three-dimensional space. All particles are arranged in some sort of Bravais lattice. We want to calculate the potential energy of a particle in this system depending on the given potential and lattice type. But before we will be able to do this calculation, some method of describing particles' spatial distribution should be developed.

We opted to use a spatial probability distribution function, further designated as $\rho(\mathbf{r})$. It answers the question what is the probability density to find some particle at (x, y, z). Moreover, it is supposed this function is not just "a collection of delta-functions", but every particle actually fluctuates near its lattice site. In terms of separate particles, it may be treated as introducing a form-factor (QFT-like approach). Regarding the whole lattice, it may be treated as a modification of Ewald's summation [11, 21] by means of introducing the ***single particle's*** probability distribution function ρ_{sp} instead of the delta-function.

Now, we directly move to calculations. It is relatively easy to introduce ρ_{sp}, at least by empirical means. But the probability distribution function ρ for the whole lattice may be a bit sophisticated. Further, we show how to "replicate" the given ρ_{sp} and construct any Bravais lattice from it. Successful usage of this method should result in something like shown in Fig. 1 (for illustrative purposes, the 2D space is shown, rather than the 3D one, as we consider).

To construct something this way, we split the whole space $\mathbb{R}^3$ into "building blocks". Let $\mathbb{V}$ designate one subset of the exact cover of $\mathbb{R}^3$ with similar domains containing strictly one particle (relative position of every particle supposed to be the same in its domain). Choice of $\mathbb{V}$ is far from being unique, but we are interested in the most natural and simple option. Thus, we will use parallelepipeds as $\mathbb{V}$ (figure 2).

One can see that choosing $\mathbb{V}$ this way satisfies all preconditions. We build a parallelepiped on Bravais lattice's base vectors, and, thus, the translation sym-

metry appears naturally. The particle is placed at the center. This is critical for subsequent calculations.

Next thing we want to do is expressing the probability distribution function ρ for the whole $\mathbb{R}^3$ through a single-particle probability distribution ρ_{sp}. It may be shown that "a slight modification" of the Fourier series can do the job. As a result, the connection between ρ and ρ_{sp} will be obtained (1)

$$\rho(\mathbf{r}) = \sum_{\mathbf{k} \in \mathbb{Z}^3} \rho_{\mathbf{k}} \mathfrak{f}_{\mathbf{k}}(\mathbf{r}), \tag{1a}$$

$$\rho_{\mathbf{k}} = \bar{\rho} \iiint\limits_{\mathbb{V}} \mathfrak{f}_{\mathbf{k}}^{*}(\mathbf{r}) \rho_{\mathrm{sp}}(\mathbf{r}) d^3\mathbf{r}, \tag{1b}$$

$$\mathfrak{f}_{\mathbf{k}}(\mathbf{r}) = e^{2\pi \mathbf{i}\left(\mathbf{k}^T \hat{G} \mathbf{r}\right)}, \tag{1c}$$

$$\hat{G} = \begin{pmatrix} \dfrac{1}{a} & -\dfrac{\cot(\alpha)}{a} & -\dfrac{\cot(\beta_c)\sin(\alpha - \alpha_c)}{a\sin(\alpha)} \\[2ex] 0 & \dfrac{\csc(\alpha)}{b} & -\dfrac{\cot(\beta_c)\sin(\alpha_c)}{b\sin(\alpha)} \\[2ex] 0 & 0 & \dfrac{\csc(\beta_c)}{c} \end{pmatrix}. \tag{1d}$$

It may be noticed that all vectors are treated as column vectors. Symbol $*$ designates here the complex conjugation, and

$$\bar{\rho} = \frac{1}{abc\sin(\alpha)\sin(\beta_c)} \tag{2}$$

is the mean particle number density. In addition, one should mention the matrix $\hat{G}$ comprising all **geometry** of the lattice under consideration.

We omit here too much detailed calculations. But referring to Appendix 6.1, one may find the proof of the ρ periodicity along vectors $\mathbf{a}$, $\mathbf{b}$, and $\mathbf{c}$. In addition, some light is shed there on the connection of the current transformation with the Fourier series and inverse lattice.

Equations (1) allow us to construct the function $\rho(\mathbf{r})$ "composed" from single particle distributions "arranged in a lattice". This principle is demonstrated by Fig. 1. Since ρ has the same symmetry as the lattice and locally is a good approximation for ρ_{sp}, it will be treated as the probability distribution function for the whole lattice.

To get a better intuitive understanding on (1) usage, one may check Example 2.2 for the Gaussian ρ_{sp}.

2.2. Example: calculating the distribution function ρ for the Gaussian single-particle distribution ρ_{sp}

We suppose that all particles are arranged in a lattice and their positions are quite determined. But since the temperature differs from zero, we can expect that particle's position fluctuates near its lattice site as (somewhat analogous to a form factor in QFT)

$$\rho_{\mathrm{sp}}(\mathbf{r}) = \frac{1}{(2\pi s^2)^{3/2}} e^{-r^2/\left(2s^2\right)}, \tag{3}$$

where s is the dispersion or localization distance by physical meaning. Equation (3) is the normal distribution, which seems to be quite reasonable for both classical and quantum (ground state of a quantum harmonic oscillator) systems.

The last assumption we do is that "Gaussian" (3) is very "sharp" and every particle lays outside the localization radius of any other particle. Otherwise, we would not be able to treat this system as a crystal in any sense. This means that s is much smaller than other characteristic distances in this system.

Now, we just plug-in $\rho_{\mathrm{sp}}(r)$ into (1b) and perform the integration. Assuming that $\rho_{\mathrm{sp}}(r)$ is a very "sharp" Gaussian, the following result is obtained:

$$\rho_{\mathbf{k}} = \bar{\rho} e^{-2\pi^2 s^2 \mathbf{k}^T \hat{G}\hat{G}^T \mathbf{k}}, \tag{4}$$

where $\bar{\rho}$ is the mean particle number density (2). For more details regarding the integration procedure, one may refer to Appendix 6.2.

Equation (4) can be directly substituted into (1a), and we will get the aimed result of this exam-
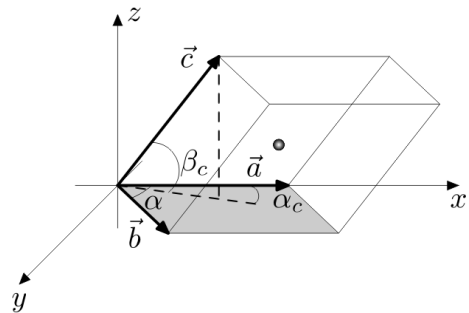

Fig. 2. One cell $\mathbb{V}$ from the exact cover of $\mathbb{R}^3$. Vectors $\mathbf{a}$, $\mathbf{b}$, and $\mathbf{c}$ are base vectors for the Bravais lattice. Angle between $\mathbf{a}$ and $\mathbf{b}$ is supposed to be α. Angle between $\mathbf{c}$ and XY plane is β_c, and the angle between its projection on XY plane and $\mathbf{a}$ is α_c. One particle is shown at the center

ple. Later, we will use (4) to calculate the potential energy for the Coulomb interaction in Subsection 2.4.

2.3. Potential energy of a single particle

Now, we switch gears to the potential energy calculation. In the regular case, one may expect i-th particle's potential energy to be something as $E_i = \sum_{j \neq i} V(r_{ij})$, where V is the interaction potential, and r_{ij} is the distance between the i- and j-th particles. But we do not want to stick to specific particles' positions and will use the probability distribution function we introduced in Subsection 2.1.

Thus, we change the summation to the integration $\sum \rightarrow \int$, and use the requirement $i \neq j \rightarrow \mathbb{R}^3 \setminus \mathbb{V}$, e.g., the exclusion of $\mathbb{V}$ that contains a particle of interest. Setting the sufficient integration borders and multiplying with the probability distribution function where needed, we get the following expression for the *single particle* potential energy E_{sp}:

$$E_{\text{sp}} = E_{\text{int}} - E_{\text{s}}, \tag{5a}$$

$$E_{\text{int}} = \iiint_{\mathbb{V}} \iiint_{\mathbb{R}^3} V\left(|\mathbf{r} - \mathbf{r}'|\right) \rho\left(\mathbf{r}\right) \rho\left(\mathbf{r}'\right) d^3\mathbf{r}' \, d^3\mathbf{r}, \tag{5b}$$

$$E_{\text{s}} = \iiint_{\mathbb{V}} \iiint_{\mathbb{V}} V\left(|\mathbf{r} - \mathbf{r}'|\right) \rho\left(\mathbf{r}\right) \rho\left(\mathbf{r}'\right) d^3\mathbf{r}' \, d^3\mathbf{r}. \tag{5c}$$

The interaction energy is presented here with $E_{\text{int}} - E_{\text{s}}$. This "splitting" is just another way of saying we want to integrate over $\mathbb{R}^3 \setminus \mathbb{V}$. If we collect both expressions (5b) and (5c) together and use $\iiint_{\mathbb{R}^3 \setminus \mathbb{V}} = \iiint_{\mathbb{R}^3} - \iiint_{\mathbb{V}}$, we will get the regular integration over $\mathbb{R}^3 \setminus \mathbb{V}$ for $\mathbf{r}'$.

In other words, Eq. (5) states following. Since the particle is localized near a lattice site, we take some "part of space" $\mathbb{V}$ around it. Then, by integration, we calculate the energy of interaction between the particle in $\mathbb{V}$ and all the rest particles in $\mathbb{R}^3 \setminus \mathbb{V}$.

Further, we call E_{int} (5b) *interaction energy* and E_{s} (5c) *self-interaction energy*. This "splitting" is convenient from the physical point of view. Basing on the nature of the considered potential, we may want or not compensate the self-interaction.

To clarify the last statement, let us consider both cases. Later on, we will analyze the Coulomb potential, and it should have definitely the self-interaction compensated. This is easily checked by considering strictly one particle: the potential energy is zero, it is

not even known whether it has some charge, because there is nothing to interact with.

A good example of when we may not want to perform the compensation is the surface distortion [11]. If the particle distorts a surface, it changes system's energy even if no other particle is present. For minimization purposes, one may "merge" this energy into the potential energy of the particle and treat this as the "self-interaction" [11]. It may be a good approach for effective interactions through a medium.

Now, we substitute (1) into (5b) to get the interaction energy in terms of the single-particle probability distribution function

$$E_{\text{int}} = \frac{1}{\bar{\rho}^2} \sum_{\mathbf{k} \in \mathbb{Z}^3} |\rho_{\mathbf{k}}|^2 \, V_{\mathbf{k}}, \tag{6a}$$

$$V_{\mathbf{k}} = \bar{\rho} \iiint_{\mathbb{R}^3} \mathfrak{f}_{\mathbf{k}}\left(\mathbf{r}'\right) V\left(|\mathbf{r}'|\right) d^3\mathbf{r}', \tag{6b}$$

where $\bar{\rho}$ is the mean particle number density. For more technical details of the performed transformation, one can refer to Appendix 6.3.

Now, we claim that (5a), (6), and (5c) are the aimed result of Section 2. The convenience of these expressions is far from being self-evident. Thus, let us consider them more carefully.

First of all, we try to handle divergences, when the system gets unbounded, and the potential is "catastrophic". Since the integration in (5c) is performed over the parallelepiped $\mathbb{V}$, and ρ_{sp} is a "good" quickly descending function, we have no divergence there. Thus, we are concerned with (6) only.

Using the Fourier series theory, one can easily show that there is only one term in (6) that can diverge, when the system gets unbounded, and the potential is "catastrophic":

$$\frac{1}{\bar{\rho}^2} |\rho_0|^2 \, V_0 = 4\pi\bar{\rho} \int\limits_0^\infty V(r) r^2 dr.$$

But this term does not contain any information on the "lattice geometry" and depends on the mean particle number density only. This means we can compare two lattices with equal mean particle number densities, even if the interparticle potential is "catastrophic". We just measure the energy from this term as ground-level (somewhat analogous to the renormalization in QFT). Now, we have tools to compare the energies of lattices and to minimize this energy with respect to lattice parameters.

The following example 2.4 shows how to calculate the potential energy for any Bravais lattice formed by charged particles. If needed, all previous calculations and following examples may be reduced to the two-dimensional case in an obvious way.

2.4. Example: calculating $E_{\mathrm{int}} - E_{\mathrm{s}}$ for screened and non-screened Coulomb potentials

Let us apply the formalism developed in Subsection 2.3 to the most interesting case of Coulomb interaction. First, we will consider the screened Coulomb potential

$$V(r) = \frac{q^2 e^{-r/\lambda_{\mathrm{D}}}}{r}, \tag{7}$$

where λ_{D} is the Debye screening distance, q is the charge of one particle. The non-screened interaction will be treated as a partial case of screened one, when $\lambda_{\mathrm{D}} \to \infty$.

We substitute V from (7) into (6b) and perform the integration to get $V_{\mathbf{k}}$

$$V_{\mathbf{k}} = \frac{4\pi\bar{\rho}q^2}{1/\lambda_{\mathrm{D}}^2 + 4\pi^2 \mathbf{k}^T \hat{G}\hat{G}^T \mathbf{k}}. \tag{8}$$

Details on how to perform this integration can be found in Appendix 6.4.

The next step is easy as well. We take (8) and substitute into (6a). One may notice that we still need $\rho_{\mathbf{k}}$ in this equation to have a complete expression for the interaction energy. As the one, we use $\rho_{\mathbf{k}}$ for the Gaussian single-particle probability distribution from Eq. (4), Example 2.2. We get

$$E_{\mathrm{int}} = \sum_{\mathbf{k}\in\mathbb{Z}^3} e^{-4\pi^2 s^2 \mathbf{k}^T \hat{G}\hat{G}^T \mathbf{k}} \frac{4\pi\bar{\rho}q^2}{1/\lambda_{\mathrm{D}}^2 + 4\pi^2 \mathbf{k}^T \hat{G}\hat{G}^T \mathbf{k}}. \tag{9}$$

For large values of λ_{D}, we will see that the first summands in (9) descend as $1/|\mathbf{k}|^2$. But if we write a series containing the interaction energy between this particle and any other straightforward, the first summands will descend only as $1/|\mathbf{k}|$. Thus, series (9) has better convergence.

To calculate the free energy with Eqs. (5), we need to find expressions for E_{int} and E_{s}. At this point, we have E_{int} (9) and still need E_{s} (5c). Let us substitute the Gaussian ρ_{sp} from (3) into (5c), take the "sharpness" of this Gaussian into account (means s is small),

and perform a simplification

$$E_{\mathrm{s}} = \frac{1}{2\sqrt{\pi}s^3} \int_0^\infty e^{-r'^2/(4s^2)} V(r') r'^2 dr'. \tag{10}$$

Then we substitute the screened Coulomb potential (7) into (10) and once more perform the integration:

$$E_{\mathrm{s}} = \frac{q^2}{\sqrt{\pi}s} - \frac{q^2}{\lambda_{\mathrm{D}}}. \tag{11}$$

Computing Eq. (11), we took again into account that s is small compared to other distances in the lattice. To see performed transformations in more details, one may use Appendix 6.5.

At this point, the expression for $E_{\mathrm{int}} - E_{\mathrm{s}}$ can be constructed from (9) and (11). One can see that, for the non-screened Coulomb potential, e.g., $\lambda_{\mathrm{D}} \to \infty$, only one term is going to infinity. It is the summand from E_{int} with $\mathbf{k} = 0$ (9). But this term does not contain $\hat{G}$. This means that there is no dependence on the lattice form, only on the mean particle number density. Thus, we can use an approach similar to the renormalization in QFT and treat this term as the "ground-level" energy. On the other hand, we can mention that it is equal to $4\pi\bar{\rho}q^2\lambda_{\mathrm{D}}^2$, which is the interaction energy with uniformly distributed charge. If we suppose that particles are in some medium with uniformly distributed charge of opposite sign, this term will be automatically equal to zero.

It may be a good point to stop, but we want to make one more step to the convergence improvement. The Coulomb interaction is very special and ubiquitous; thus, it looks reasonable to search for as good approximation for particle energy as possible. If we introduce the mean distance between particles,

$$l = \frac{1}{\sqrt[3]{\bar{\rho}}}, \tag{12}$$

and suppose that the lattice is not degenerate, then Eq. (10) can be approximated as

$$E_{\mathrm{int}} - E_{\mathrm{s}} = \frac{\sqrt{\pi}q^2}{l} \sum_{\mathbf{k}\neq 0} \frac{e^{-\mathbf{k}^T \hat{G}^{-1T}\hat{G}^{-1}\mathbf{k}/l^2}}{\mathbf{k}^T \hat{G}^{-1T}\hat{G}^{-1}\mathbf{k}/l^2} +$$

$$+ \frac{q^2}{\pi l} \sum_{\mathbf{k}\neq 0} \frac{e^{-l^2 \mathbf{k}^T \hat{G}\hat{G}^T \mathbf{k}}}{l^2 \mathbf{k}^T \hat{G}\hat{G}^T \mathbf{k}} - \frac{2\sqrt{\pi}q^2}{l} + 4\pi\bar{\rho}q^2\lambda_{\mathrm{D}}^2. \tag{13}$$

More details on the approximation procedure can be found in Appendix 6.6.

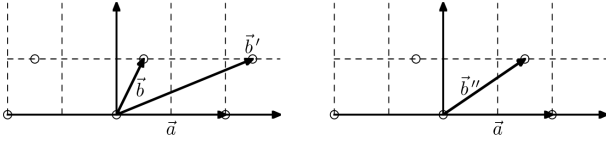**Fig. 3.** Same lattice in different representations. It has translation symmetry with respect to two vectors **a** and **b**. Left figure shows different choices for the second translation vector: **b** and **b'**. Using reflections, one may show that the lattice on the right is the same as the left one. So, **b''** is a possible choice as well. When performing the numerical calculations, additional restrictions are used to overcome this uncertainty

One may see that the last term is equal to the energy in the case of evenly distributed charge. It is very useful to note that this is the only summand that approaches infinity, if $\lambda_D \to \infty$. This means that (13) can be used for the comparison of different lattices even without screening. We will only need to measure the energy, by starting from $4\pi\bar{\rho}q^2\lambda_D^2$ as "ground-level". Other terms are corrections due to the charge pointness and comprise all information on the lattice geometry.

Now, the last self-check. The Coulomb interaction is long-range, and the localization distance s should not play any significant role in the approximation. Here, we see that it is really absent. Rather different may be a picture for short-range interactions or effective interactions with uncompensated E_s.

The obtained equation (13) is, in some sense, equivalent to Ewald's series – same idea of splitting into two sums over the lattice and over inverse lattice and the same convergence rate. But the Ewald summation implies some arbitrary constants that are chosen experimentally, depending on a specific lattice, to achieve a better performance. Methods of choosing these parameters are significantly different in different works [38–45]. In the present contribution, we obtain series without any "free variables". If needed, the Reader may treat the presented derivation as the construction of Ewald series with all parameters "built-in" and tuned for for the best performance in the scope of the considered problem.

There is one more thing to point out. We do not focus on calculating the potential energy itself – this is rather a byproduct. What we want is *comparing* two lattices; we only need "<" or ">" sign to put lattices in order. This means that even if the obtained series are not "overprecise" compared to different approaches, they are extremely useful. As we will see

further, the obtained series are "order-preserving" and allow us to compute the lattice parameters with less than 100 summands per lattice.

3. Using Lattice Symmetry When Performing the Computer Minimization of the Potential Energy

Here, we develop a method for examining the potential energy of one particle from an infinite Bravais lattice. We want this method to be suitable for the minimization of this energy with respect to lattice parameters.

It looks like Eqs. (6) and (5c) or their specific version for the Coulomb interaction (13) should be enough. But one who tries to minimize the potential energy within numerical methods will meet the following problem. All possible parameter values (translation vectors) and all possible Bravais lattices are not in the one-to-one correspondence. There is an infinite set of possible triples of -translation vectors that describe the same Bravais lattice.

Performing the potential energy minimization, a computer searches for a triple of translation vectors that should be substituted into the expression for $E_{int} - E_s$ to obtain a minimal possible value. But, due to the mentioned uncertainties, one starts sometimes to choose triples containing longer and longer vectors. This is so, because the calculation errors emerge, and the algorithm starts thinking that longer vectors make the potential energy smaller. Thus, it is highly desirable to somehow restrict parameters and remove uncertainties from the choice of translation vectors.

In Section 3, we will analyze possible uncertainties and provide a method to avoid the mentioned problem during the minimization.

It is easier to start with a 2D lattice. Figure 3 shows the uncertainty, when choosing parameters. One may see that it can be eliminated, if we claim that the projection of **b** on **a** is less than a half of **a**. In terms of parameters, this may be expressed as

$$0 \le b\cos(\alpha) \le \frac{a}{2}. \tag{14}$$

Restrictions in the 3D case are more sophisticated. To imagine the translation vectors, one can refer to Fig. 2. Obviously, (14) should be kept for 3D, as is. We only need the additional consideration for **c**.

The definition of vector **c** has same problems as **b** in Fig. 3 has had. For any Bravais lattice, **c** can be

chosen so that its projection is inside of the parallelogram built on **a** and **b**. This conclusion becomes obvious after considering Fig. 2 and thinking about **c** in the same manner, as about **b** in Fig. 3.

But, using the reflection with respect to the XY plane, this condition may be strengthened. Considering Fig. 4, one may see that **c** may be always projected to the lower part of the parallelogram constructed on **a** and **b**. Using the expression for the mean particle number density (2), we get

$$c_x = c\cos(\beta_c)\cos(\alpha_c) = \frac{\cot(\beta_c)\cos(\alpha_c)}{\bar\rho ab\sin(\alpha)},$$

$$c_y = c\cos(\beta_c)\sin(\alpha_c) = \frac{\cot(\beta_c)\sin(\alpha_c)}{\bar\rho ab\sin(\alpha)}.$$

Then, by adding the restriction mentioned above, we have

$$0 < c_y < \frac{b\sin(\alpha)}{2},$$
$$c_y\cot(\alpha) < c_x < c_y\cot(\alpha) + a. \tag{15}$$

Equations (14) and (15) are enough to set up a one-to-one correspondence between translation vectors and Bravais lattices. They will be used in Section 4 to get the parameters of a dust crystal with minimal potential energy.

4. Grains in Dusty Plasma, Dust Crystal, and Its Lattice

It is known that grains in dusty plasma interact and even show the self-organization in form of the melting and the crystallization of dust crystals [16–20]. We aim to apply the methods developed in Section 2 to this system. As the first approximation, we suppose that grains interact only as charged particles (screened Coulomb potential). The obtained equation (13) (example 2.4) allows us to calculate the energy of any lattice just inserting the correct matrix $\hat G$ and performing the summation. But much more interesting is finding the lattice with minimal energy, when the particle number density $\bar\rho$ is fixed. The obtained result can be verified experimentally.

We will perform the minimization of the potential energy with respect to $\hat G$ parameters, if the mean particle number density is constant. The expression for $E_{\rm sp} \equiv E_{\rm int} - E_{\rm s}$ was already obtained as (13), example 2.4. Moreover, the problem of different $\hat G$ representing the same lattice is solved by introducing restrictions (14) and (15) in Section 3.
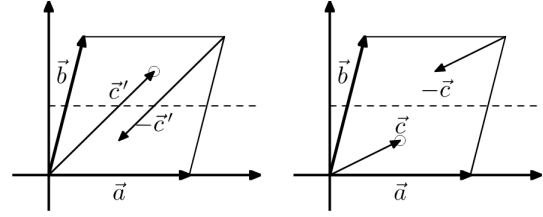
Fig. 4. Projection of the same lattice in different representations on the XY plane. The particles from layers above and below the XY plane are shown by a circle and a filled circle, respectively. Particles in the XY plane are not explicitly shown. If a particle from above the plane is projected into the upper half of the ab parallelogram, a reflection with respect to the XY plane can be used to get representation, where this particle is in the lower half of the parallelogram

To simplify the minimization, we perform few transformations of (13). First of all, we designate $a = l(1+\delta a)$, $b = l(1+\delta b)$, and express c through (2). One may notice that l is canceled out in exponents and denominators in (13). This means that the used method of minimization allows us to cancel out the mean interparticle distance and leads to the scale-free minimization. This result is significant on its own – we claim that the lattice predicted during the minimization does not depend on the mean particle density. This agrees with the physical intuition, since the Coulomb interaction is long-range and does not contain any specific distance parameters. Second, it allows us to work with numbers that are comfortable for a computer and do not cause too big calculation errors. In the same way, we perform manipulations on restrictions (14) and (15). One should see that we have obtained this restrictions in a way that preserves scale-free properties of the equations.

In addition, we mention that we need to minimize only parts with $\hat G$ and, thus, disregard other terms in $E_{\rm int} - E_{\rm s}$ (this is proper, because the particle number density is constant). Now, the only term containing l is q/l in the expression for $E_{\rm int} - E_{\rm s}$. But it can be factored out and, thus, does not affect the minimization – we just ignore it.

The numerical minimization was performed with the standard function FindMinimum of Wolfram Mathematica v.9. Both sums in (13) are highly convergent. Thus, we can limit the summation with $|\mathbf{k}| \le 4$. Taking more summands does not change the calculated optimal lattice.

Now, we can present the results of numerical minimization in Fig. 5 and Table.
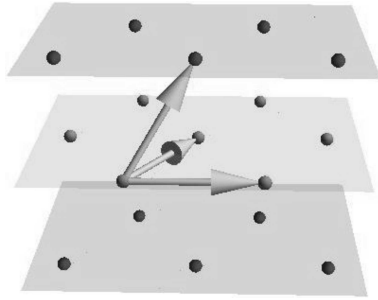
Fig. 5. Part of the lattice obtained by the minimization. As is seen, the 3D lattice consists of interleaving planes with 2D hexagonal (triangular) lattices in each. The only difference between planes is a shift: particles from one plane are projected onto "empty spaces" in another one. Translation vectors are shown as well

Parameter	Calculated value	Hexagonal close packing (HCP)
α	≈ 1.04717	$\pi/3 \approx 1.0472$
α_c	≈ 0.523589	$\pi/6 \approx 0.5236$
β_c	≈ 0.955205	$\arcsin(\sqrt{2/3}) \approx 0.9553$
a	≈ 1.122462	$\sqrt[6]{2} \approx 1.12246$
b	≈ 1.122462	$\sqrt[6]{2} \approx 1.12246$

Looking at Fig. 5, one may see that it is very similar to a hexagonal close-packed (HCP) lattice. HCP consists of two interleaving planes with a triangular 2D lattice in each as well. So, we may check, if this is really the HCP lattice, by comparing their parameters.

The results show that the lattice obtained by numerical calculations is really HCP. This complies with experimental data and the computer simulation [16, 17].

5. Conclusions

In conclusion, we want to make some overview of the results we have obtained.

In Section 2, we have developed a general formalism for calculations of the potential energy. Any Bravais lattice can be treated within this approach, even if the interparticle potential is "catastrophic". As the most interesting example, the Coulomb potential was considered (both screened and non-screened). In the following sections, this result was used to find which lattice is formed by dust particles in plasma.

The obtained equations are, in some sense, equivalent to Ewald's series – the same idea of splitting into two sums over the lattice and over the inverse lattice; the same convergence rate. But the Ewald summation implies some arbitrary constants that are chosen experimentally depending on a specific lattice to achieve the better performance. The methods of choosing these parameters may be significantly different in different works [38–45]. In the present work, we have obtained series without any "free variables". If needed, the Reader may treat the presented derivation as obtaining the Ewald series with all prameters "built-in" and tuned for for the best performance in the scope of the considered problem.

We do not focus on calculating the potential energy itself – this is rather a byproduct. What we want is the comparison of two lattices; we only need the $<$ or $>$ sign to put lattices in order. This means that even if the obtained series are not "overprecise" compared to different approaches, they are extremely useful. As is shown, the obtained series are "order-preserving" and allow one to compute lattice parameters with less than 100 summands per lattice.

But even having the expression for potential energy, one will face the problem of ambiguity of the choice of translation vectors, when describing some Bravais lattice. During a numerical computation, this may cause the algorithm to choose longer and longer translation vectors. This is because the calculation errors emerge, and the algorithm starts thinking that longer vectors make the potential energy smaller. In Section 3, we have developed methods to overcome this problem. As a result, a restriction on translation vectors is obtained. This restriction allows us to eliminate the uncertainty and to perform the minimization correctly. Moreover, the obtained restrictions, as well as series for the minimization, are "scale-free", which has positive effect on computations.

Section 4 is devoted to the consideration of dusty plasma. We use the results from the previous sections to find out what is the lattice type of a dust crystal. It seems we should expect a hexagonal close-packed (HCP) lattice for grains in dusty plasma. This result is independent on grains' charge unless they all are equally charged. In addition, there is no dependence on the screening distance, if only it is larger than the mean interparticle distance. This coincides with the results of other numerical simulations [17] and experiments [16]. The above result has been obtained, by

using less than 100 summands per lattice. Thus, we treat the performed calculations as "near-analytical" and leaving a possibility to find sometime a fully analytical approach to this class of problems.

6. APPENDICES

During this article, we tried to provide the rigorous exposition of presented ideas, but without physical sole being lost in lots of equations. Thus, calculations that heavily rely on mathematical transformations only were moved to appendices. The Reader interested only in "physical part" may omit them.

6.1. On the properties of $\mathfrak{f}_\mathbf{k}(\mathbf{r})$

In (1), we present how to calculate the probability distribution function for the whole system $\rho(\mathbf{r})$ basing on the single-particle probability distribution function $\rho_{\mathrm{sp}}(\mathbf{r})$. It is based on the decomposition of ρ_{sp}, by using $\mathfrak{f}_\mathbf{k}(\mathbf{r})$ (1c) as basis functions in the inverse lattice space. Here, we add some consideration about the connection between a Fourier series and the presented one.

Suppose we have a function $g(\mathbf{u})$ defined on the unit cube $\mathbb{U} \equiv [0;1] \times [0;1] \times [0;1]$. This function can be expressed in terms of a Fourier series

$$g(/bfu) = \sum_{\mathbf{k} \in \mathbb{Z}^3} g_\mathbf{k}\, e^{2\pi \mathrm{i}(\mathbf{k}^T \mathbf{u})},$$
$$g_\mathbf{k} = \iiint_\mathbb{U} g(\mathbf{u}) e^{-2\pi \mathrm{i}(\mathbf{k}^T \mathbf{u})} d^3\mathbf{u}. \tag{16}$$

Let us consider a bijection $\hat{G}$ (1d) from $\mathbb{V}$ to $\mathbb{U}$ and its inverse $\hat{G}^{-1} : \mathbb{U} \to \mathbb{V}$ (see Fig. 2 for a geometrical reasoning)

$$\hat{G}^{-1} = \begin{pmatrix} a & b\cos(\alpha) & c\cos(\alpha_c)\cos(\beta_c) \\ 0 & b\sin(\alpha) & c\sin(\alpha_c)\cos(\beta_c) \\ 0 & 0 & c\sin(\beta_c) \end{pmatrix}. \tag{17}$$

It may be seen that the rows of $\hat{G}$ are components of the inverse lattice basis vectors. We are interested in the case $g(\mathbf{u}) = \rho_{\mathrm{sp}}(\hat{G}^{-1}\mathbf{u})$. Since we know that $\forall \mathbf{r} \in \mathbb{V} : \rho_{\mathrm{sp}}(\hat{G}^{-1}\hat{G}\mathbf{r}) = \rho_{\mathrm{sp}}(\mathbf{r})$, one can immediately write

$$\rho_{\mathrm{sp}}(\mathbf{r}) = \sum_{\mathbf{k} \in \mathbb{Z}^3} g_\mathbf{k} e^{2\pi \mathrm{i}(\mathbf{k}^T \hat{G}\mathbf{r})}. \tag{18}$$

In the same way, we consider the second equation from (16):

$$g_\mathbf{k} = \iiint_\mathbb{V} \rho_{\mathrm{sp}}(\hat{G}^{-1}\mathbf{u}) e^{-2\pi \mathrm{i} \mathbf{k}^T \hat{G}\hat{G}^{-1}\mathbf{u}} \frac{d^3(\hat{G}^{-1}\mathbf{u})}{J[\hat{G}^{-1}\mathbf{u}]}, \tag{19}$$

where J is a Jacobian. Here, $\hat{G}^{-1}\mathbf{u}$ is treated as a new variable with the domain $\mathbb{V}$.

The Jacobian $J[\hat{G}^{-1}\mathbf{u}] = abc\sin(\alpha)\sin(\beta_c) = 1/\bar{\rho}$ is actually the volume of $\mathbb{V}$ or the inverse mean particle number density. Designating $g_\mathbf{k}$ as $\rho_\mathbf{k}$ in (18) and (19), changing the variable in (19) $\hat{G}^{-1}\mathbf{u} \to \mathbf{r}$, and designating the exponent in (18) as $\mathfrak{f}_\mathbf{k}$ (it can be seen that the exponent in (19) is $\mathfrak{f}_\mathbf{k}^*$, where

$*$ designates the complex conjugation), we immediately get Eqs. (1). Moreover, the obtained result means that all properties of a Fourier series can be applied to decomposition (1).

The last thing to be mentioned is periodical properties of the presented series. We are going to expand the domain to $\mathbb{R}^3$ so that $\rho(\mathbf{r})$ will be defined everywhere in the space. Now, we need to explore the behavior of this function. From (1d), one may see that, if $l \in \mathbb{Z}$, $m \in \mathbb{Z}$, and $n \in \mathbb{Z}$,

$$\hat{G}(\mathbf{r} + l\mathbf{a} + m\mathbf{b} + n\mathbf{c}) = \hat{G}\mathbf{r} + l\mathbf{e}_x + m\mathbf{e}_y + n\mathbf{e}_z, \tag{20}$$

where $\mathbf{e}_x$, $\mathbf{e}_y$, and $\mathbf{e}_z$ are unit vectors along the coordinate axes. With regard for (1c), we have

$$\mathfrak{f}_\mathbf{k}(\mathbf{r} + l\mathbf{a} + m\mathbf{b} + n\mathbf{c}) = \mathfrak{f}_\mathbf{k}(\mathbf{r}) \tag{21}$$

and, from (1a),

$$\rho(\mathbf{r} + l\mathbf{a} + m\mathbf{b} + n\mathbf{c}) = \rho(\mathbf{r}). \tag{22}$$

The last equation justifies our view of the connection between ρ and ρ_{sp}, as it is presented in Fig. 1.

6.2. On the expression of $\rho_\mathbf{k}$ for the Gaussian ρ_{sp}

We suppose that $\rho_{\mathrm{sp}}(\mathbf{r})$ is either 0 everywhere in $\mathbb{R}^3 \setminus \mathbb{V}$ or at least negligibly small. If so, we can change the integration limits in (1b) to infinite ones.

At this point, we are interested in a specific form of ρ_{sp} (3); thus, it is explicitly substituted into (1b). In addition, we designate $\vec{\mathcal{K}} = 2\pi \mathbf{k}^T \hat{G}$ and rewrite the expression in Cartesian coordinates, by changing the multiple integral to the product of integrals

$$\rho_\mathbf{k} = \frac{\bar{\rho}}{(2\pi s^2)^{3/2}} \prod_{j=1}^{3} \int_{-\infty}^{\infty} e^{-r_j^2/(2s^2) - \mathrm{i}\mathcal{K}_j r_j}\, dr_j.$$

The last expression can be integrated, if we use the relation [31]

$$\int_{-\infty}^{+\infty} e^{-p^2 x^2 \pm qx}\, dx = \frac{\sqrt{\pi}}{p} e^{q^2/(2p)^2}, \quad \Re(p^2) > 0.$$

As a result, we get

$$\rho_\mathbf{k} = \bar{\rho} \prod_{j=1}^{3} e^{-\mathcal{K}_j^2 s^2/2}\, dr_j.$$

Changing the product of exponents to the exponent of a sum and mentioning that $\sum_j \mathcal{K}_j^2 = \vec{\mathcal{K}}\vec{\mathcal{K}}^T = 4\pi^2 \mathbf{k}^T \hat{G}\hat{G}^T \mathbf{k}$, we immediately get (4).

6.3. On the expression of E_{int}

Let us start with (5b). The inner integral has infinite limits. So, we may rewrite this expression as follows:

$$E_{\mathrm{int}} = \iiint_\mathbb{V} \iiint_{\mathbb{R}^3} V(|\mathbf{r}'|)\, \rho(\mathbf{r})\, \rho(\mathbf{r} + \mathbf{r}')\, d^3\mathbf{r}'\, d^3\mathbf{r}.$$

Since $\rho(\mathbf{r})$ is real, it can be replaced with complex conjugate $\rho^*(\mathbf{r})$ without changing E_{int}. Now, we can substitute ρ from (1a) and mention that $\mathfrak{f}_{\mathbf{k}}(\mathbf{r} + \mathbf{r}') = \mathfrak{f}_{\mathbf{k}}(\mathbf{r})\,\mathfrak{f}_{\mathbf{k}}(\mathbf{r}')$ (1c). If we designate $V_{\mathbf{k}}$ as in (6b), it can be written as

$$E_{\text{int}} = \frac{1}{\bar{\rho}} \sum_{\mathbf{k} \in \mathbb{Z}^3} \rho_{\mathbf{k}} V_{\mathbf{k}} \sum_{\mathbf{k}' \in \mathbb{Z}^3} \rho_{\mathbf{k}'}^* \iiint_{\mathbb{V}} \mathfrak{f}_{\mathbf{k}}(\mathbf{r})\, \mathfrak{f}_{\mathbf{k}'}^*(\mathbf{r})\, d^3\mathbf{r}.$$

The last equation can be simplified, if we perform the integration. From Appendix 5, we expect the orthogonality of $\mathfrak{f}_{\mathbf{k}}$ functions. From (1c), we have $\mathfrak{f}_{\mathbf{k}}(\mathbf{r})\mathfrak{f}_{\mathbf{k}'}^*(\mathbf{r}) = \mathfrak{f}_{\mathbf{k}-\mathbf{k}'}(\mathbf{r})$, and we get

$$\iiint_{\mathbb{V}} \mathfrak{f}_{\mathbf{k}}(\mathbf{r})\mathfrak{f}_{\mathbf{k}'}^*(\mathbf{r})\, d^3\mathbf{r} = abc\sin(\alpha)\sin(\beta_c)\delta_{\mathbf{k},\mathbf{k}'}. \tag{23}$$

Here, $\delta_{\mathbf{k},\mathbf{k}'} = \delta_{k_x,k_x'}\delta_{k_y,k_y'}\delta_{k_z,k_z'}$ is a product of three Kronecker's deltas.

Mentioning that $abc\sin(\alpha)\sin(\beta_c) = 1/\bar{\rho}$, where $\bar{\rho}$ is the mean particle number density (one particle per $\mathbb{V}$, see fig. 2 for a geometrical reasoning), we get (6a).

6.4. $V_{\mathbf{k}}$ for the screened Coulomb potential

Let us consider Eqs. (1c) and (1d) in spherical coordinates

$$\mathfrak{f}_{\mathbf{k}}(\mathbf{r}) = e^{2\pi i r \left(g_{\mathbf{k}}\cos(\theta) + g_{\mathbf{k}}'\cos(\varphi - \delta\varphi_{\mathbf{k}})\sin(\theta)\right)},$$

$$g_{\mathbf{k}} = \frac{k_x \sin(\alpha_c - \alpha)}{a\tan(\beta_c)\sin(\alpha)} - \frac{k_y \sin(\alpha_c)}{b\tan(\beta_c)\sin(\alpha)} + \frac{k_z}{c\sin(\beta_c)},$$

$$g_{\mathbf{k}}' = \sqrt{\frac{k_x^2}{a^2} + \left(\frac{k_y}{b\sin(\alpha)} - k_x \frac{\cot(\alpha)}{a}\right)^2},$$

and rewrite $V_{\mathbf{k}}$ from (6b)

$$V_{\mathbf{k}} = \bar{\rho} \int_0^{\infty} dr V(r) r^2 \times$$

$$\times \int_0^{\pi} d\theta \sin(\theta) \underbrace{\int_0^{2\pi} d\varphi\, e^{2\pi i r\left(g_{\mathbf{k}}\cos(\theta) + g_{\mathbf{k}}'\cos(\varphi - \delta\varphi_{\mathbf{k}})\sin(\theta)\right)}}_{I(\theta)}.$$

Integrating over φ, we get

$$I(\theta) = 2\pi e^{2\pi i g_{\mathbf{k}} r \cos(\theta)} J_0\left(2\pi g_{\mathbf{k}}' r \sin(\theta)\right).$$

Then we substitute the last expression into the equation for $V_{\mathbf{k}}$

$$V_{\mathbf{k}} = 2\pi\bar{\rho} \int_0^{\infty} V(r) r^2 \int_0^{\pi} e^{2\pi i g_{\mathbf{k}} r \cos(\theta)} \times$$

$$\times J_0\left(2\pi g_{\mathbf{k}}' r \sin(\theta)\right) \sin(\theta) d\theta dr.$$

We will consider the screened Coulomb potential (7), which means that the integration over r can be performed. One may use the relation [31]

$$\int_0^{\infty} e^{-\alpha x} J_\nu(\beta x) x^{\nu+1} dr = \frac{2\alpha(2\beta)^\nu \Gamma\left(\nu + \frac{3}{2}\right)}{\sqrt{\pi}(\alpha^2 + \beta^2)^{\nu+3/2}},$$

$$\Re(\alpha) > |\Im(\beta)|, \Re(\nu) > -1$$

and combine it with the equation for $V_{\mathbf{k}}$ to get

$$V_{\mathbf{k}} = \int_0^{\pi} \frac{2\pi\bar{\rho}q^2\left(1/\lambda_{\mathrm{D}} - 2\pi i g_{\mathbf{k}}\cos(\theta)\right)\sin(\theta)d\theta}{\left(\left(1/\lambda_{\mathrm{D}} - 2\pi i g_{\mathbf{k}}\cos(\theta)\right)^2 + \left(2\pi g_{\mathbf{k}}'\sin(\theta)\right)^2\right)^{3/2}}.$$

Changing the variable $t = \cos(\theta)$ and performing the integration over t, we will get

$$V_{\mathbf{k}} = \frac{4\pi\bar{\rho}q^2}{1/\lambda_{\mathrm{D}}^2 + 4\pi^2 g_{\mathbf{k}}^2 + 4\pi^2 g_{\mathbf{k}}'^2}.$$

The last expression is equivalent to (8). One may check this by expanding $g_{\mathbf{k}}$ and $g_{\mathbf{k}}'$.

6.5. Calculation of E_{s} for the screened Coulomb potential

We will start with Eq. (5c) and assume that ρ_{sp} is a very "sharp" function (example 2 2.2). With this assumption, we can change the integration limits to infinite ones. In turn, this will allow us to perform a change of the variable, as we did in (5):

$$E_{\mathrm{s}} = \iiint_{\mathbb{R}^3} \iiint_{\mathbb{R}^3} V(|\mathbf{r}'|)\rho_{\mathrm{sp}}(\mathbf{r})\rho_{\mathrm{sp}}(\mathbf{r} + \mathbf{r}')d^3\mathbf{r}'\, d^3\mathbf{r}. \tag{24}$$

First of all, we perform some mathematical transformations with (3) (in the Cartesian coordinate system) and get

$$\rho_{\mathrm{sp}}(\mathbf{r})\rho_{\mathrm{sp}}(\mathbf{r} + \mathbf{r}') = \frac{1}{8\pi^3 s^6} e^{-\left[\mathbf{r} + \mathbf{r}'/2\right]^2/s^2 - \mathbf{r}'^2/(4s^2)}.$$

Now, we substitute this expression into (24) and perform the integration over $\mathbf{r}$. Writing the result in a spherical coordinate system and integrating over angles, we immediately get (10).

Since we know the explicit expression for V (7), we can substitute it into (10) and perform the integration, by using the definition of the complementary error function [32]

$$\mathrm{erfc}(x) = \frac{2}{\sqrt{\pi}} \int_x^{\infty} e^{-t^2} dt. \tag{25}$$

As a result, we get

$$E_{\mathrm{s}} = \frac{q^2}{\sqrt{\pi}s}\left(1 - \frac{s\sqrt{\pi}}{\lambda_{\mathrm{D}}} e^{s^2/\lambda_{\mathrm{D}}^2}\mathrm{erfc}(s/\lambda_{\mathrm{D}})\right). \tag{26}$$

We may obviously suppose that s is very small compared to the screening distance. Then $s \ll \lambda_{\mathrm{D}}$. So, we can approximate the last equation and, as a result, get (11).

6.6. Approximation of $E_{\mathrm{int}} - E_{\mathrm{s}}$ for the screened Coulomb potential

We start with expression (9) for E_{int}. But one may see that it contains the expressions $s^2\hat{G}$ and $\hat{G}^T$. Components of the $\hat{G}\hat{G}^T$ matrix in (9) are proportional to various products of inverse distances in a lattice, e.g., $1/a^2$, $1/(ab)$, and so on (see (1d)). Since $s \ll a$, $s \ll b$, and $s \ll c$ (assumption about "sharp Gaussian"), we expect $\left|s^2\hat{G}\hat{G}^T\right| \ll 1$. This means that the exponent "starts acting" only for terms with very large

$|\mathbf{k}|$. In this section, we will try to rewrite the equations to get even a better convergence than we have.

First of all, we rewrite the expression for E_{int} as follows:

$$E_{\text{int}} = \frac{2\bar{\rho}q^2}{\pi} e^{s^2/\lambda_{\text{D}}^2} \int\limits_{2\pi s}^{\infty} \mathfrak{s}\, e^{-\mathfrak{s}^2/(2\pi\lambda_{\text{D}})^2} \sum_{\mathbf{k}\in\mathbb{Z}^3} e^{-\mathfrak{s}^2\mathbf{k}^T\hat{G}\hat{G}^T\mathbf{k}} d\mathfrak{s}.$$

One may easily integrate this expression and check that it is equal to (9).

We note that the variable $\mathfrak{s}$ takes values much smaller than the mean distance (12), as well as much bigger. Thus, we split this integral into two. First integration is executed from $2\pi s$ to l and the second one from l to infinity.

We assume that the lattice is not too degenerate (Section 2 2.4), which means that the angles α and β_c should not significantly differ from $\pi/2$. So, we may expect elements of $\mathfrak{s}^2\hat{G}\hat{G}^T$ to be less than 1 for the first integral and greater than 1 for the second one. If so, then the second integration may be performed, and we end up with the sum that converges much better than (9),

$$E_{\text{int}} = \frac{2\bar{\rho}q^2}{\pi} e^{s^2/\lambda_{\text{D}}^2} \int\limits_{2\pi s}^{l} \mathfrak{s}\, e^{-\mathfrak{s}^2/(2\pi\lambda_{\text{D}})^2} \underbrace{\sum_{\mathbf{k}\in\mathbb{Z}^3} e^{-\mathfrak{s}^2\mathbf{k}^T\hat{G}\hat{G}^T\mathbf{k}}}_{\Theta(0;\mathfrak{s}^2\hat{G}\hat{G}^T)} d\mathfrak{s} +$$

$$+ 4\pi\bar{\rho}q^2 \sum_{\mathbf{k}\in\mathbb{Z}^3} \frac{e^{s^2/\lambda_{\text{D}}^2 - l^2\left(1/[2\pi\lambda_{\text{D}}]^2 + \mathbf{k}^T\hat{G}\hat{G}^T\mathbf{k}\right)}}{1/\lambda_{\text{D}}^2 + 4\pi^2\mathbf{k}^T\hat{G}\hat{G}^T\mathbf{k}}.$$

From (1d), one may check with Sylvester's criterion [33] that $\hat{G}$ (1d) is a positive definite matrix. Obviously, we expect $\hat{G}^T$ and their product $\hat{G}\hat{G}^T$ to be positive definite matrices as well. Since $\mathfrak{s}$ takes only positive values, $\mathfrak{s}^2\hat{G}\hat{G}^T$ is positive as well. This means the highlighted sum in the last equation is the Riemann theta function [34] at the point $z = 0$. So, we appropriately designate it with $\Theta\left(0; \mathfrak{s}^2\hat{G}\hat{G}^T\right)$.

Using the modular transformation [34]

$$\Theta(z;\hat{A}) = \frac{\pi^{d/2}}{\sqrt{\det\hat{A}}}\Theta(\hat{A}^{-1}z;\hat{A}^{-1}), \tag{27}$$

where d is the number of dimensions (3 in this case), we get

$$\Theta\left(0;\mathfrak{s}^2\hat{G}\hat{G}^T\right) = \frac{\pi^{3/2}}{\mathfrak{s}^3\det\hat{G}}\Theta\left(0;\hat{G}^{-1\,T}\hat{G}^{-1}/\mathfrak{s}^2\right).$$

We used the fact that $\det\hat{G} = \det\hat{G}^T$ and that the multiplication by $\mathfrak{s}^2$ is equal to the multiplication by a diagonal matrix, which has all elements equal to $\mathfrak{s}^2$. The explicit expression for $\hat{G}^{-1}$ may be used from (17). In addition, we note that

$$\det\hat{G} = \frac{1}{abc\sin(\alpha)\sin(\beta_c)} = \bar{\rho} \tag{28}$$

and rewrite the expression for E_{int} as

$$E_{\text{int}} = 2\sqrt{\pi}q^2 e^{s^2/\lambda_{\text{D}}^2} \sum_{\mathbf{k}\in\mathbb{Z}^3} \underbrace{\int\limits_{2\pi s}^{l} e^{-\mathfrak{s}^2/(2\pi\lambda_{\text{D}})^2 - |\hat{G}^{-1}\mathbf{k}|^2/\mathfrak{s}^2}\frac{d\mathfrak{s}}{\mathfrak{s}^2}}_{I(\mathbf{k})} +$$

$$+ 4\pi\bar{\rho}q^2 \sum_{\mathbf{k}\in\mathbb{Z}^3} \frac{e^{s^2/\lambda_{\text{D}}^2 - l^2\left(1/[2\pi\lambda_{\text{D}}]^2 + |\hat{G}^T\mathbf{k}|^2\right)}}{1/\lambda_{\text{D}}^2 + 4\pi^2\mathbf{k}^T\hat{G}\hat{G}^T\mathbf{k}}.$$

Now, we can perform the integration and find $I(\mathbf{k})$. Since the result is very complicated, we introduce two helper functions

$$\phi(L) = \frac{e^{-L^2/(2\pi\lambda_{\text{D}})^2}}{L} - \frac{1}{2\sqrt{\pi}\lambda_{\text{D}}}\operatorname{erfc}\left(\frac{L}{2\pi\lambda_{\text{D}}}\right),$$

$$f_\alpha(L) = e^{\alpha|\hat{G}^{-1}\mathbf{k}|/(\pi\lambda_{\text{D}})}\operatorname{erfc}\left[\frac{|\hat{G}^{-1}\mathbf{k}|}{L} + \frac{\alpha L}{2\pi\lambda_{\text{D}}}\right],$$

and present the result in terms of these functions as

$$I(\mathbf{k} = 0) = \phi(2\pi s) - \phi(l),$$
$$I(\mathbf{k} \neq 0) = \sqrt{\pi}\left(f_{-1}(l) - f_{-1}(2\pi s)\right)/\left|4\hat{G}^{-1}\mathbf{k}\right| +$$
$$+ \sqrt{\pi}\left(f_{+1}(l) - f_{+1}(2\pi s)\right)/\left|4\hat{G}^{-1}\mathbf{k}\right|.$$

Using the precise expression (26) for E_{s}, one may get

$$E_{\text{s}} = 2\sqrt{\pi}q^2 e^{s^2/\lambda_{\text{D}}^2}\phi(2\pi s).$$

So, subtracting E_{s} from E_{int} simply means the neglect of this term.

Our previous calculations do not rely on any approximation, but the expression for $I(\mathbf{k} \neq 0)$ is very complicated, so we need to perform one. Before we do, one should show it is acceptable to approximate this sum. Subsequent calculations are divided into two parts: *uniform convergence proof* and *approximation* itself.

Proof of uniform convergence. We will use the Cauchy criterion for the sequence of functions $f_i(x)$ in the domain E to achieve this goal: $\forall\varepsilon > 0\ \exists N\ \forall m \geq n > N : \forall x \in E : \left|\sum_{i=n}^{m} f_i(x)\right| < \varepsilon$. Further, $\sum_{\mathbf{k}\in\mathbb{Z}^3} I(\mathbf{k})$ acts as a sequence for the checking of convergence and the entries of $\hat{G}^{-1}$, as well as s, l, and λ_{D} are treated as variables from the domain of admissible parameters. We have already examined properties of $\hat{G}^{-1}$ and will not get into details again.

First of all, we use $s < l < \lambda_{\text{D}}$. This relation holds for the physical system under consideration, and we will use it in all subsequent calculations. This means $f_\alpha(l) > f_\alpha(2\pi s)$. Thus, all terms in the sum will be positive, and we can avoid using the absolute value. The second thing that appears is the following bound:

$$0 < \sum_{\mathbf{k}\in\mathbb{Z}^3\setminus\{\mathbf{0}\}} I(\mathbf{k}) < \sum_{\mathbf{k}\in\mathbb{Z}^3\setminus\{\mathbf{0}\}} \frac{f_{-1}(l) + f_{+1}(l)}{\left|4\hat{G}^{-1}\mathbf{k}\right|}\sqrt{\pi}.$$

Then we use relation $\operatorname{erfc}(x) \leq e^{-x^2}$ for $x > 0$ [35] and replace erfc in $f_{\pm 1}(l)$. Expanding the squares in exponents and performing a simplification, we get

$$\sum_{\mathbf{k}\in\mathbb{Z}^3\setminus\{\mathbf{0}\}} I(\mathbf{k}) < \sum_{\mathbf{k}\in\mathbb{Z}^3\setminus\{\mathbf{0}\}} \frac{\exp\left(-\frac{|\hat{G}^{-1}\mathbf{k}|^2}{l^2} - \frac{l^2}{4\pi^2\lambda_{\text{D}}^2}\right)}{\left|\hat{G}^{-1}\mathbf{k}\right|}.$$

In addition, $2\sqrt{\pi} < 4$ was used.

Now, we can use the known relation $\min_{\|\mathbf{x}\|_2=1} \|\hat{A}\mathbf{x}\|_2 = \sqrt{\lambda_{\min}}$, where $\lambda_{\min}$ is the minimal eigenvalue of $\hat{A}^\dagger \hat{A}$, and $\dagger$ designates the Hermitian adjoint [36]. We know that $\det \hat{G}^{-1} = 1/\bar{\rho} > 0$. Thus, $\hat{G}^{-1\dagger}\hat{G}^{-1}$ has nonzero eigenvalues. Taking the minimal $\lambda_{\min}$ and designating $g = \sqrt{\lambda_{\min}}$, we claim $\left|\hat{G}^{-1}\mathbf{k}\right| \geq g\,|\mathbf{k}|$.

Now, we should change the multidimensional summation to a one-dimensional one. Since all summands are positive, we can rearrange them in any convenient order. Thus, we will perform the summation over "cube surfaces". First of all, let us designate

$$\mathbb{K}_n = \left\{\mathbf{k} \in \mathbb{Z}^3 \,\middle|\, |k_x| \leq n \wedge |k_y| \leq n \wedge |k_z| \leq n\right\}.$$

Then the total sum can be expressed as

$$\sum_{\mathbf{k} \in \mathbb{Z}^3 \setminus \{\mathbf{0}\}} I(\mathbf{k}) = \sum_{n=1}^{+\infty} \sum_{\mathbf{k} \in \mathbb{K}_n \setminus \mathbb{K}_{n-1}} I(\mathbf{k}),$$

where the number of summands in $\mathbb{K}_n \setminus \mathbb{K}_{n-1}$ can be easily calculated as $(2n+1)^3 - (2n-1)^3 \equiv 24n^2 + 2$. The minimal length for the index vector in this set of indices is n.

Collecting together the results of previous calculations, we get

$$\sum_{\mathbf{k} \in \mathbb{Z}^3 \setminus \mathbb{K}_m} I(\mathbf{k}) < \sum_{n=m+1}^{+\infty} \frac{(24n^2 + 2)\exp\left(-\frac{g^2 n^2}{l^2} - \frac{l^2}{4\pi^2 \lambda_{\mathrm{D}}^2}\right)}{gn}.$$

The further proof is supposed to be obvious, and, thus, we avoid it. The proof of uniform convergence for the first summand in E_{int} can be performed much more easily by the presented scheme and, thus, it is avoided as well. Instead, one useful remark should be done. The series converges better, when g/l is bigger. Taking the physical meaning of these variables into account, we get following statement: if we project the vectors $\mathbf{a}$, $\mathbf{b}$, and $\mathbf{c}$ on the axes X, Y, and Z, respectively (see Fig. 2) and divide by the mean distance in the lattice $1/\sqrt[3]{\bar{\rho}}$, we will get measure of how a good current series converges or, by the physical meaning, how close is the lattice to a cubic one.

Approximation. We take into account that $s \ll l \ll \lambda_{\mathrm{D}}$, neglect all terms containing l/λ_{D} and s/λ_{D} in erfc, and approximate $\mathrm{erfc}(x \to \infty)$ by $\sim e^{-x^2}/(x\sqrt{\pi})$ [37]. Obviously, $f_\alpha(l) \gg f_\alpha(2\pi s)$, and, thus, all f with $2\pi s$ arguments are neglected. In addition, we neglect all small terms in the exponent and denominators. To make this procedure more clear, we state $\left|\hat{G}^{-1}\mathbf{k}\right|/l > l/\lambda_{\mathrm{D}}$. It means that the screening distance is big enough not to feel a deviation of the lattice from a cubic one. This leads us to the equations

$$\phi(l) \approx \frac{1}{l}, \quad I(\mathbf{k} \neq 0) \approx \frac{l}{2\left|\hat{G}^{-1}\mathbf{k}\right|^2} e^{-\left|\hat{G}^{-1}\mathbf{k}\right|^2/l^2}.$$

To get the first one, the identity $\mathrm{erfc}(x) = 1 - \mathrm{erf}(x)$ and the approximation $\mathrm{erf}(x \to 0) \sim 2x/\sqrt{\pi}$ [37] were used.

Now, the approximate equation (13) can be written.

1. V.E. Fortov, A.V. Ivlev, S.A. Khrapak, A.G. Khrapak, G.E. Morfill. Complex (dusty) plasma: Current status, open issues, perspectives. *Phys. Rep.* **421**, 1 (2005) [DOI: 10.1016/j.physrep.2005.08.007].

2. H. Löwen. Melting, freezing and colloidal suspensions. *Phys. Rep.* **237**, 249 (1994) [DOI: 10.1016/0370-1573(94)90017-5].

3. G.E. Morfill, H.M. Thomas, U. Konopka, M. Zuzic. The plasma condensation: Liquid and crystalline plasmas. *Phys. Plasmas* **6**, 1769 (1999) [DOI: 10.1063/1.873435].

4. Y. Bilotsky. On calculation of lattice energy in spatially confined domains. *Advances in Materials Science and Applications* **2**, (4), 127 (2013).

5. L.N. Kantorovich, I.I. Tupitsyn. Coulomb potential inside a large finite crystal. *J. Phys.: Condens. Matter* **11**, 6159 (1999).

6. L.P. Buhler, R.E. Crandal. On the convergence problem for lattice sums. *J. Phys. A: Math. Gen.* **23**, 2523 (1990) [DOI: 10.1088/0305-4470/23/12/029].

7. D. Borwein, J.M. Borwein, R. Shail, I.J. Zucker. Energy of static electron lattices. *J. Phys. A: Math. Gen.* **20**, 1519 (1988) [DOI: 10.1088/0305-4470/21/7/015].

8. T.R.S. Prasanna. Physical meaning of the Ewald sum method. *Phil. Magaz. Lett.* **92**, No. 1, 29 (2012) [DOI: 10.1080/09500839.2011.622725].

9. Y. Bilotsky, M. Gasik. A new approach for modelling lattice energy in finite crystal domains. *Phys.: Conf. Ser.* **633**, 012014 (2015) [DOI: 10.1088/1742-6596/633/1/012014].

10. D.M. Heyes, A.C. Braṅka. Lattice summations for spread out particles: Applications to neutral and charged systems. *J. Chem. Phys.* **138**, 034504 (2013) [DOI: 10.1063/1.4775367].

11. B.I. Lev, V.P. Ostroukh, V.B. Tymchyshyn, A.G. Zagorodny. Statistical description of the system electrons on the liquid helium surface. *Eur. Phys. J. B* 87:253 (2014) [DOI: 10.1140/epjb/e2014-50303-2].

12. D. Ruelle. *Statistical Mechanics: Rigorous Results* (Benjamin, 1969).

13. A. Isihara. *Statistical Mechanics* (Academic Press, 1971).

14. K. Huang. *Statistical Mechanics* (Wiley, 1963).

15. R. Baxter. *Exactly Solved Models in Statistical Mechanics* (Academic Press, 1982).

16. B. Klumov, G. Joyce, C. Räth, P. Huber, H. Thomas, G.E. Morfill, V. Molotkov, V. Fortov. Structural properties of 3D complex plasmas under microgravity conditions. *Europhys. Lett.* **92** (1), 15003 (2010) [DOI: 10.1209/0295-5075/92/15003].

17. B.A. Klumov, G.E. Morfill. Structural properties of complex (dusty) plasma upon crystallization and melting. *JETP Lett.* **90** (6), 444 (2009) [DOI: 10.1134/S002136400918009X].

18. B.I. Lev, A.G. Zagorodny. Structure formation in system of Brownian particle in dusty plasma. *Phys. Lett. A* **373**, 1101 (2009) [DOI: 10.1016/j.physleta.2009.01.044].

19. B.I. Lev, V.B. Tymchyshyn, A.G. Zagorodny. Brownian particle in non-equilibrium plasma. *Condens. Phys.* **12**, 593 (2009) [DOI: 10.5488/CMP.12.4.593].

20. H. Thomas, G.E. Morfill, V. Demmel, J. Goree, B. Feuerbacher, D. Mohlmann. Plasma crystal: Coulomb crystal-

lization in a dusty plasma. *Phys. Rev. Lett.* **73**, 652 (1994) [DOI: 10.1103/PhysRevLett.73.652].

21. P. Ewald. Die Berechnung optischer und elektrostatischer Gitterpotentiale. Ann. Phys. **369** (3), 253 (1921) [DOI: 10.1002/andp.19213690304].

22. J.H. Chu, Lin I. Direct observation of Coulomb crystals and liquids in strongly coupled rf dusty plasmas. *Phys. Rev. Lett.* **72**, 4009 (1994) [DOI: 10.1103/ PhysRevLett.72.4009].

23. A. Melzer, T. Trottenberg, A. Piel. Experimental determination of the charge on dust particles forming Coulomb lattices. *Phys. Lett. A* **191**, 301 (1994) [DOI: 10.1016/0375-9601(94)90144-9].

24. S.V. Vladimirov, S.A. Khrapak, M. Chaudhuri, G.E. Morfill. Superfluidlike motion of an absorbing body in a collisional plasma. *Phys. Rev. Lett.* **100**, 055002 (2008) [DOI: 10.1103/PhysRevLett.100.055002].

25. H. Ikezi. Coulomb solid of small particles in plasmas. *Phys. Fluids* **29**, 1764 (1986) [DOI: 10.1063/1.865653].

26. A. Melzer, A. Homann, A. Piel. Experimental investigation of the melting transition of the plasma crystal. *Phys. Rev. E* **53**, 2757 (1996) [DOI: 10.1103/PhysRevE.53.2757].

27. A.G. Sitenko, A.G. Zagorodny, V.N. Tsytovich. Fluctuation phenomena in dusty plasmas. *AIP Conf. Proc.* **345**, 311 (1995) [DOI: 10.1063/1.49020].

28. S.A. Brazovsky. Phase transition of an isotropic system to a nonuniform state. *Sov. Phys. JETP* **41** (1), 85 (1975).

29. B.I. Lev, H. Yokoyama. Selection of states and fluctuation under the first order phase transitions. *Int. J. Mod. Phys. B* **17**, 4913 (2003) [DOI: 10.1142/S021797920302274X].

30. H. Totsuji, T. Kishimoto, C. Totsuji. Structure of confined Yukawa system (dusty plasma). *Phys. Rev. Lett.* **78**, 3113 (1997) [DOI: 10.1103/PhysRevLett.78.3113].

31. I.S. Gradshteyn, I.M. Ryzhik. *Tables of Integrals, Series, and Products* (Academic Press, 2007).

32. A. Erdélyi, W. Magnus, F. Oberhettinger, F. G. Tricomi. *Higher Transcendental Functions* (Krieger, 1981), Vol. 2.

33. R. Bellman. *Introduction to Matrix Analysis* (Society for Industrial and Applied Mathematics, 1970).

34. R. Bellman. *A Brief Introduction to Theta Functions* (Holt, Rinehart and Winston, 1961).

35. M. Chiani, D. Dardari, M.K. Simon. New exponential bounds and approximations for the computation of error probability in fading channels. *IEEE Transactions on Wireless Communications* **4** (2), 840 (2003) [DOI: 10.1109/ TWC.2003.814350].

36. C. Meyer. *Matrix Analysis and Applied Linear Algebra* (SIAM, 2000).

37. M. Abramowitz, I. Stegun. *Handbook of Mathematical Functions with Formulas, Graphs, and Mathematical Tables* (Dover, 1974).

38. B.R. Brooks, R.E. Bruccoleri, B.D. Olafson, D.J. States, S. Swaminathan, M. Karplus. HARMM: A program for macromolecular energy, minimization, and dynamics calculations. *J. Comput. Chem.* **4**, 187 (1983) [DOI: 10.1002/ jcc.540040211].

39. T. Darden, D. York, L. Pederson. Particle mesh Ewald: An $N \cdot \log(N)$ method for Ewald sums in large systems. *J. Chem. Phys.* **98**, 10089 (1993) [DOI: 10.1063/1.464397].

40. B. Nijboer, E. De Wette. On the calculation of lattice sums. *Physica* **23**, 309 (1957) [DOI: 10.1016/S0031-8914(57)92124-9].

41. J. Kolafa, J. Perram. Cutoff errors in the Ewald summation formulae for point charge systems. *Mol. Simulation* **9**, 351 (1992) [DOI: 10.1080/08927029208049126].

42. J. Perram, H. Petersen, S. De Leeuw. An algorithm for the simulation of condensed matter which grows as the 3/2 power of the number of particles. *Mol. Phys.* **65**, 875 (1988) [DOI: 10.1080/00268978800101471].

43. Z. Rycerz, P. Jacobs. Ewald summation in the molecular dynamics simulation of large ionic systems. *Mol. Simulation* **8**, 197 (1992) [DOI: 10.1080/08927029208022476].

44. W. Smith. FORTRAN code for the Ewald summation method. *Information Quarterly for Computer Simulation of Condensed Phases* **21**, 37 (1986).

45. D. York, W. Yang. The fast Fourier Poisson method for calculating Ewald sums. *J. Chem. Phys.* **101**, 3298 (1994) [DOI: 10.1063/1.467576].

Б.I. Лев, В.Б. Тимчишин, А.Г. Загородній

АНАЛІЗ ПОТЕНЦІАЛЬНОЇ ЕНЕРГІЇ
СИСТЕМИ ВЗАЄМОДІЮЧИХ ЧАСТИНОК,
УПОРЯДКОВАНИХ У ҐРАТКУ БРАВЕ

Р е з ю м е

Запропоновано метод визначення типу ґратки, утвореної порошинками у запиленій плазмі та оцінки їх потенціальної енергії. Основоположною складністю цієї задачі є міжчастинковий потенціал, що відноситься до "катастрофічних". Такі потенціали потребують особливих підходів, щоб уникнути розбіжностей в процесі обчислення потенціальної енергії. У даній роботі розвинено необхідну для поставленої мети модифікацію відповідних методів. Показано, що отримані таким чином вирази для потенціальної енергії можна застосувати для визначення параметрів ґратки, а також, що знайдені значення параметрів відповідають відомим експериментальним даним.